Meteorologische Zeitschrift, Vol. **XX**, No. X, 1-3 (April 20XX)

Article

Intercomparison of integrated water vapour measurements

LORENZ MARTIN[1,*], CHRISTIAN MÄTZLER[1], TIM J. HEWISON[2], DOMINIQUE RUFFIEUX[3]

[1]Institute of Applied Physics, University of Bern, Switzerland
[2]Met Office, University of Reading, UK
[3]MeteoSwiss, Payerne, Switzerland

(Manuscript received June XX, XXXX; in revised form October XX, XXXX; accepted November XX, XXXX)

Abstract

Measurements of tropospheric integrated water vapour (IWV) made with two microwave radiometers (ASMUWARA, TP/WVP-3000), GPS, and radiosondes (SRS 400) during the Temperature, hUmidity, and Cloud (TUC) profiling campaign under mid-latitude conditions in Payerne, Switzerland, in winter 2003/2004 are compared. All methods provide robust IWV retrievals in clear sky and cloudy situations. The mean difference between radiometric and radiosonde IWV is less than 0.15 kgm^{-2} being not significant with respect to the standard deviation and to the theoretical accuracy. The GPS IWV measurements have a persistent significant dry bias of approx. 0.5 kgm^{-2} with respect to radiometers and radiosondes. The different temporal and spatial resolutions of the instruments were found to have a strong influence on the standard deviation. A characteristic diurnal cycle of the GPS and radiometric IWV was observed.

Zusammenfassung

Der troposphärische integrierte Wasserdampf (IWV) wurde mit zwei Mikrowellenradiometern (ASMUWARA, TP/WVP-3000), GPS und Radiosonden (SRS 400) während der Temperature, hUmidity, and Cloud (TUC) profiling Kampagne in mittlerer geographischer Breite in Payerne, Schweiz, im Winter 2003/2004 gemessen und verglichen. Alle Methoden haben sich sowohl bei klarem Himmel wie auch bei Bewölkung bewährt. Die mittlere Differenz zwischen radiometrischem und Radiosonden-IWV ist weniger als 0.15 kgm^{-2}. Dies ist nicht signifikant mit Bezug auf die Standardabweichung und auf die theoretische Genauigkeit. Der mit GPS bestimmte IWV hat einen beständigen systematischen Fehler von ca. -0.5 kgm^{-2} mit Bezug auf die Radiometer und auf die Radiosonden. Es wurde festgestellt, dass die unterschiedliche zeitliche und örtliche Auflösung der Instrumente einen starken Einfluss auf die Standardabweichung hat. Ein charakteristischer Tagesgang des radiometrischen und des GPS-IWV wurde beobachtet.

1 Introduction

The concentration of water vapour in the troposphere is typically approx. 1%, but its impact on physical processes in the troposphere is outstanding. Water vapour is the most important greenhouse gas, and the change between its gaseous, liquid and solid state is an effective means of energy storage and transport in local and global weather. Thus it is crucial in meteorology to know its amount and its distribution precisely.

This is one of the reasons why the COST 720 Temperature, hUmidity, and Cloud (TUC) profiling campaign (RUFFIEUX et al. (2006)) was held at the aerological station of MeteoSwiss in Payerne, Switzerland, in winter 2003/2004. The station is located close to the Lake of Neuchâtel at 490 m above sea level where weather situations with fog and temperature inversions occur frequently during winter. A database of meteorological measurements made with in-situ and various remote sensing methods was produced to asses their potential for tropospheric monitoring under these conditions. Whereas CIMINI et al. (2006) investigated the retrieval of humidity and temperature profiles, this paper focuses on integrated water vapour (IWV). Three methods were used for the retrieval of IWV in the TUC campaign: radiosondes, the global positioning system (GPS), and two different types of microwave radiometers. Since the radiometers also measure the integrated liquid water (ILW), these data are included in the intercomparison.

Similar studies were made by EMARDSON et al. (1998) and by KOPKEN (2001) within the Baltic Sea Experiment (BALTEX) and by REVERCOMB et al. (2003) within the Atmospheric Radiation Measurement (ARM) programme. However, this study is the first to involve IWV measurements made with the SRS 400 radiosonde (RICHNER (1999)) and with the All-Sky MUlti WAvelength RAdiometer (ASMUWARA, MARTIN et al. (2006a)). Furthermore, the all-sky scanning capabilities of ASMUWARA are used to asses the influence of inhomogeneities in the water vapour field on the IWV measurement.

Fig. 1 shows an overview of the IWV dataset gained

*Corresponding author: Lorenz Martin, Institute of Applied Physics, University of Bern, Sidlerstrasse 5, CH-3012 Bern, Switzerland, e-mail: lorenz.martin@mw.iap.unibe.ch

0941-2948/XX/00XX-XXXX $ X.XX
DOI: 10.1127/0941-2948/20XX/00XX-XXXX

during the TUC campaign spanning 108 days from 5th Nov. 2003 to 23rd Feb. 2004. The mean IWV value of this period was 10.2 kgm^{-2}, and the lowest and the highest values were around 2 kgm^{-2} and 20 kgm^{-2}, respectively. This range is typical for the winter season at mid-latitudes. The plot also shows that the measurements match well in general (note that the data from the four instruments are plotted in the order of the plot legend and that some values are concealed).

2 Instruments

2.1 Radiosondes

The radiosondes used for the intercomparison were SRS 400 manufactured by Meteolabor AG (RICHNER (1999)). These radiosondes are equipped with a copper-constantan thermocouple and a Sippican resisitive hygristor for the temperature and humidity measurement, respectively. The hygristor has a slow response time especially at temperatures below $-30°$C. Furthermore, the humidity measurement was found to have systematic errors. For that reason, some radiosondes were equipped with additional chilled-mirror hygrometers (FUJIWARA et al. (2003); VÖMEL et al. (2003)) to deduce a correction algorithm. This correction was applied on the TUC dataset and increased the radiosonde IWV by typ. 5% (RUFFIEUX et al. (2006)). Since the humidity sensor of the radiosondes only works between the ground and the tropopause (10493 m above ground on average for TUC), a standard profile (KNEIZYS et al. (1996)) was used above. However, the effect of this correction being less than 0.01 kgm^{-2} is negligible. The radiosondes were regularly launched at 11:00 UT and 23:00 UT, and some extra launches were made at 05:00 UT and at 17:00 UT resulting in totally 254 launches. The ascent to the tropopause took 31 min on average.

2.2 GPS derived IWV

By measuring the propagation time taken by a microwave signal on the way from a GPS satellite to a GPS receiver, the position of the receiver can be determined. The propagation of the GPS signal through the atmosphere is delayed by several effects including water vapour. Knowing the position of a fixed ground-based receiver, the delay caused by the water vapour can be calculated and the IWV is directly inferred (BEVIS et al. (1992)). The GPS IWV in the TUC campaign was available as hourly averages. The Niell mapping function (NIELL (1996)) was used to obtain zenith values from measurements made at 10° minimum elevation angle.

2.3 ASMUWARA radiometer

ASMUWARA (All-Sky MUlti WAvelength RAdiometer) is a ground-based ten-channel microwave and infrared radiometer system (MARTIN et al. (2006a)) designed to retrieve temperature and humidity profiles, cloud parameters, and IWV and ILW. The channels used for the IWV and ILW retrieval are at 23.60 GHz near the centre of a water vapour absorption line and at 31.50 GHz in an atmospheric window sensible to water clouds, respectively. Both radiometer channels are calibrated with tipping scans. The IWV and ILW are deduced with a linear combination of the opacities measured at these two frequencies. The coefficients of the linear functions were computed from radiative transfer simulations based on a one-year dataset of radiosonde launches from Payerne (totally 720, MARTIN et al. (2006a,b); ELGERED et al. (1982)). ASMUWARA has a half-power full beam width of approx. 8.5°. A special feature of ASMUWARA is its ability to measure IWV and ILW in all directions of the upper hemisphere. However, only zenith measurements made approx. every 100 s were used in the intercomparison. This selection is favourable for the comparison with the TP/WVP-3000 radiometer (cf. Sec. 2.4), but has drawbacks in terms of radiometric noise and for the comparison with GPS data as will be discussed in Sec. 5. All tipping scans in W direction were ruled out due to an artificial signal causing excess IWV. Measurements made during rain and other spurious data were cleared from the dataset.

2.4 TP/WVP-3000 radiometer

The TP/WVP-3000 by Radiometrics Corp. is a commercial twelve-channel microwave radiometer capable of retrieving profiles of temperature and humidity as well as IWV and ILW (WARE et al. (2003)). Radiometrics' retrieval is based on a standard feed forward neural network with input, hidden, and output layers and with full connection between adjacent layers. The twelve microwave radiometer channels as well as surface temperature, humidity and pressure and infrared brightness temperature are used as input. The neural network was trained a priori using a standard back propagation algorithm with a dataset of ten years of high resolution radiosondes from Payerne. Values were excluded from the dataset when the built-in rain sensor of the TP/WVP-3000 detected rain. The TP/WVP-3000 channels primarily contributing to the IWV and ILW measurement are calibrated with tipping scans and have a half-power full beam width of approx. 5.5°. Measurements made in zenith direction at intervals of typ. 5 min were used for the intercomparison.

3 Intercomparison

The data compared in the following are from the whole TUC campaign. Measurements made at day and at night

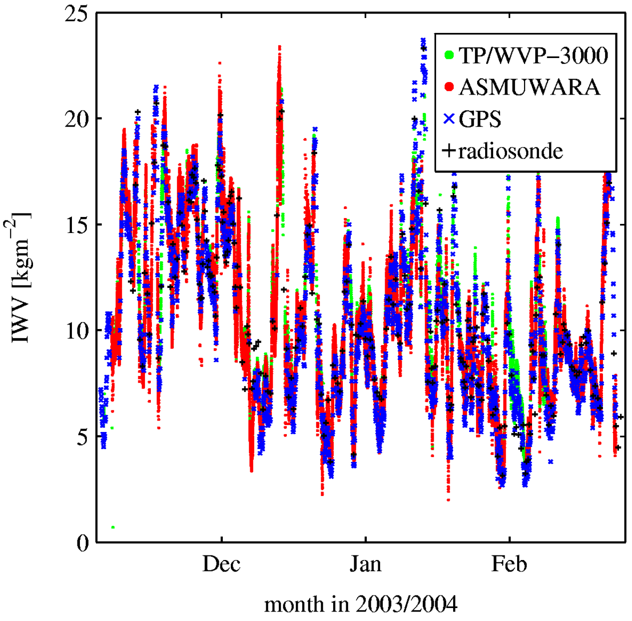

Figure 1: Overview of the IWV measurements made with two radiometers (TP/WVP-3000 and ASMUWARA), GPS, and radiosondes during the TUC campaign in winter 2003/2004 in Payerne, Switzerland

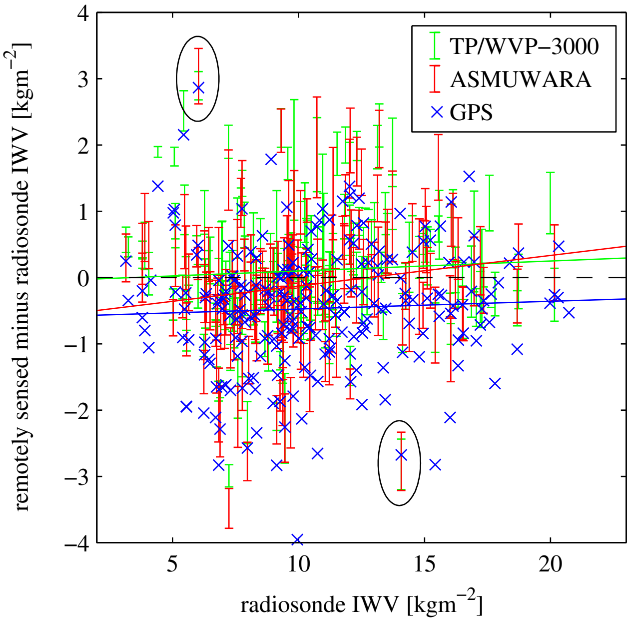

Figure 2: TP/WVP-3000, ASMUWARA, and GPS derived IWV minus radiosonde derived IWV. The error bars mark the double standard deviation of the radiometer data averaged over the time of the corresponding radiosonde ascent. The black ellipses mark two samples where the radiosonde has a strong bias with respect to the three other instruments. Numerical values are given in Table 1.

	TP/WVP-3000	ASMUWARA	GPS
samples	183	169	204
mdiff [kgm^{-2}]	0.11	−0.12	−0.47
std [kgm^{-2}]	0.93	0.96	0.96
sed [kgm^{-2}]	0.07	0.07	0.07
mstd [kgm^{-2}]	0.16	0.21	
slope	0.01	0.05	0.01
corr	0.97	0.97	0.97

Table 1: Numerical values to Fig. 2. samples: number of samples; mdiff: mean difference; std: standard deviation; sed: standard error; mstd: mean std of all averaging intervals; slope: slope of fitted straight line; corr: correlation coefficient.

as well as measurements made under cloudy and clear-sky conditions are considered. Because rain strongly affects the radiometric measurements, the tipping-bucket rain sensor at Payerne and the rain sensor of the TP/WVP-3000 were used to exclude rainy periods from the dataset (approx. 30% of the data, including data rejected due to instruemntal failure). In an additional screening, pairs of data with differences of more than 4 times the standard deviation were rejected (approx. 2% of the data). Most of these outliers were due to intermittent rain or appeared at the beginning or at the end of rainy periods.

3.1 Radiosondes, GPS and Radiometers

In a first step, the radiosonde measurements were compared with the three other instruments. The IWV mean values and standard deviations (std) from the radiometers were determined over the radiosonde ascent time, and the GPS measurements were selected so that a temporal overlap of at least 15 min was achieved. Fig. 2 shows TP/WVP-3000, ASMUWARA, and GPS derived IWV minus radiosonde IWV vs. radiosonde IWV, and Table 1 gives the corresponding numerical values. It is seen that the scatter is large, and that the mean difference is smaller than the std. With respect to the standard error of the difference (sed, std divided by the square root of the number of samples), the mean difference between radiometers and radiosondes is not significant to the 2-sed level, whereas the difference between GPS and radiosonde IWV has a dry bias. The std of a single averaging interval (error bars in Fig. 2) is a measure of the temporal humidity fluctuation and of the radiometric noise and drift during that interval. Small std's indicate good radiometer performance and/or stable atmospheric conditions. The mean std of all averaging intervals, i. e. the mean of the error bars in Fig. 2 is larger than the mean difference also implying a non significant bias between the radiometers and the radiosondes. The radiosonde measurement has the tendency to underestimate high IWV values and to overestimate low IWV values, most distinctly in comparison with ASMUWARA.

The overall impression is that the radiosondes give consistent IWV values on average, but when taking single ascents, the difference to other instruments can be considerable. This is illustrated with the two ellipses in Fig. 2 where the IWV measurements of TP/WVP-3000, ASMUWARA, and GPS match very well, but the deviation from the radiosonde IWV is almost 3 kgm^{-2}. This

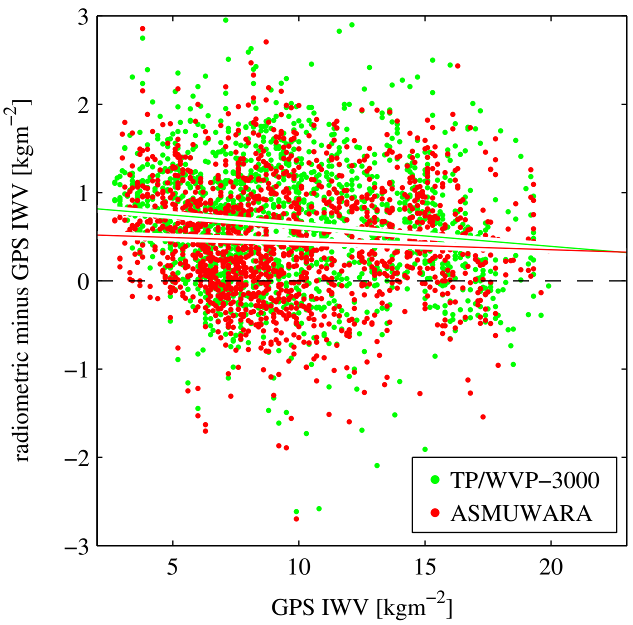

Figure 3: TP/WVP-3000 and ASMUWARA derived IWV minus GPS derived IWV. Numerical values are given in Table 2.

	TP/WVP-3000	ASMUWARA
samples	1643	1534
mdiff [kgm^{-2}]	0.63	0.45
std [kgm^{-2}]	0.70	0.67
mstd [kgm^{-2}]	0.22	0.27
slope	−0.02	−0.01
corr	0.98	0.98

Table 2: Numerical values to Fig. 3. samples: number of samples; mdiff: mean difference; std: standard deviation; mstd: mean std of all averaging intervals; slope: slope of fitted straight line; corr: correlation coefficient.

value is almost an order of magnitude larger than the 5% error of the radiosonde measurement (RUFFIEUX et al. (2006)). The deviations may be due to calibration problems of the radiosondes, but even more probably to the different temporal and spatial sampling of the methods as will be discussed in Sec. 5.

3.2 GPS and Radiometers

In a next step, GPS derived IWV was compared with measurements of the two radiometers. Since the GPS data are provided on hourly basis, the radiometer data were averaged over the respective hours of the GPS values. Radiometric IWV minus GPS derived IWV is shown in Fig. 3 (note that the ordinate has a different scale than in Fig. 2) along with numerical values in Table 2. Similarly to the findings of the previous section, the GPS IWV has a dry bias of approx. 0.54 kgm^{-2} with respect to the two radiometers, and the bias is smaller than the std.

The dry bias was also observed in other comparison studies. LIOU et al. (2001) reported a similar dry bias in

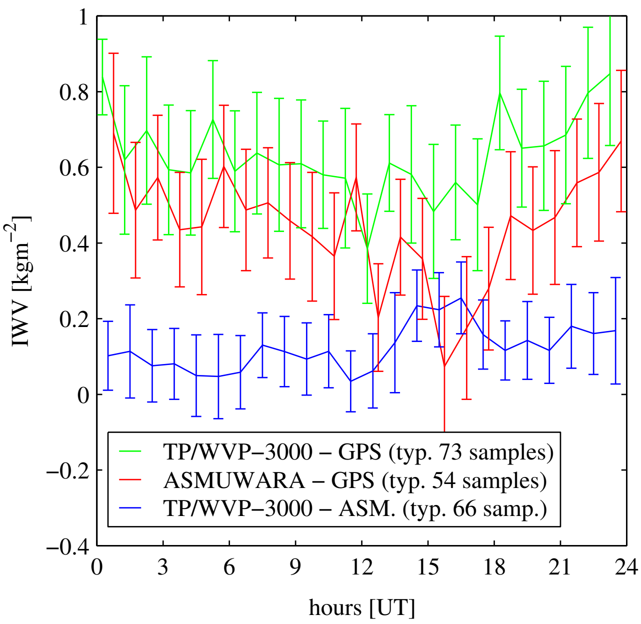

Figure 4: Hourly IWV differences between two instruments, averaged over the time of the whole TUC campaign. The error bars mark the double standard error.

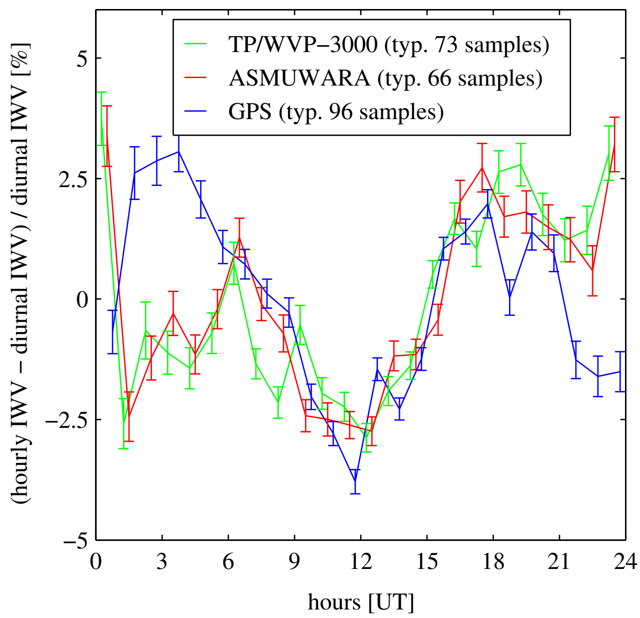

Figure 5: Hourly IWV means minus diurnal IWV means divided by diurnal IWV means in %, averaged over the time of the whole TUC campaign. The error bars mark the double standard error.

a campaign in Taipei, Taiwan. Comparisons made during the ARM programme (REVERCOMB et al. (2003)) produced a dry bias of approx. 1 kgm^{-2}, and EMARDSON et al. (1998) stated a dry bias of 1.3 kgm^{-2}. However, EMARDSON et al. (1998) used GPS receivers with radomes causing additional signal delay resulting in excess IWV. Furthermore, it should be borne in mind that the measurements of the TUC campaign were made during winter and that the IWV values are larger in summer presumably leading to a larger dry bias. TREGONING et al. (1998) noticed that the GPS dry bias is more distinct for high IWV values, whereas the results presented here are opposite (Figures 2 and 3).

To find reasons for the dry bias, the diurnal variations of the IWV was analysed more closely. Fig. 4 shows hourly averages of the difference between measurements of two instruments and the corresponding sed averaged over the time of the whole campaign. The dry bias of the GPS measurement is again well visible. Whereas the IWV difference between the radiometers is almost constant except for a peak in the afternoon, the IWV difference between GPS and the radiometers is more variable and has a distinct maximum at midnight. This could be the result of extra refraction of GPS signals by the enhanced inversions more prevalent at night. The hourly mean IWV minus diurnal mean IWV divided by the diurnal mean IWV averaged over the time of the whole TUC campaign is shown in Fig. 5. It is seen that the diurnal evolution coincides in the daytime and that the GPS measurement is more variable with respect to the radiometric measurement at night. A similar diurnal evolution was found by GUEROVA et al. (2005) where GPS measurements and calculations from a numerical weather prediction model showed a minimum at noon. The diurnal cycle is possibly due to insufficient modelling of the effective tropospheric temperature (MARTIN et al. (2006a); WANG et al. (2005)). However, the interpretation of the diurnal cycle and especially the variability of the GPS IWV at night remains difficult to understand. Furthermore, the observed diurnal effects are close to the measurement uncertainties.

3.3 ASMUWARA and TP/WVP-3000

Finally, IWV measurements from ASMUWARA and from TP/WVP-3000 were compared (Fig. 6 and Table 3). The data were averaged over thirty-minute intervals based on typ. 16 ASMUWARA measurements and on typ. 6 TP/WVP-3000 measurements. Because the data considered for the intercomparison contain zenith values only and due to the shorter averaging interval, the std is considerably smaller than in the intercomparisons of Sections 3.1 and 3.2. Despite the smaller std the mean difference between ASMUWARA and TP/WVP-3000 is not significant. The mean difference as well as the std and the mean std are smaller than the theoretical accuracy of 0.5 kgm^{-2} achievable for a single measurement (MARTIN et al. (2006b)). The correlation is close to 1 and the slope of the fitted straight line is consistent with the value from Sec. 3.2 (note that the ordinate has a different scale than in Figures 2 and 3). The largest discrepancies occur for IWV values larger than 18 kgm^{-2}. An inspection of these data revealed them being due to two 5-hour-periods on 9$^{\text{th}}$ Nov. and 13$^{\text{th}}$ Dec.

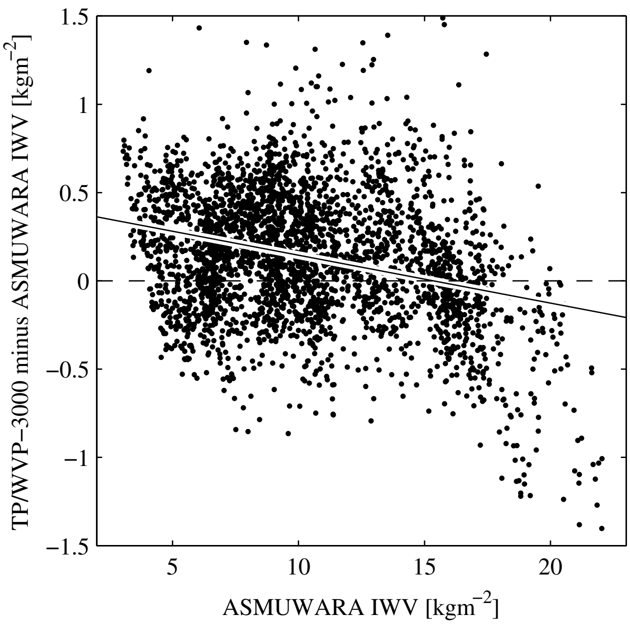

Figure 6: TP/WVP-3000 derived IWV minus ASMUWARA derived IWV. Numerical values are given in Table 3.

	TP/WVP-3000
samples	3072
mdiff [kgm^{-2}]	0.14
std [kgm^{-2}]	0.37
mstd [kgm^{-2}]	0.15
corr	0.996
slope	−0.03

Table 3: Numerical values to Fig. 6. samples: number of samples; mdiff: mean difference; std: standard deviation; mstd: mean std of all averaging intervals; slope: slope of fitted straight line; corr: correlation coefficient.

2003, respectively. Whereas in the first, clear-sky period the IWV increased and decreased rapidly, the IWV rose and declined more slowly in the second period having light clouds. Both periods were not affected by rain. Since another four periods with IWV values larger than 18 kgm^{-2} did not show large discrepancies, it is difficult to spot a systematic error for large IWV values. However, ASMUWARA seems to have suffered from radiometric non-linearities as shown by CIMINI et al. (2006) in an analysis of brightness temperatures. The radiometric non-linearities were eliminated after the TUC campaign.

3.4 Integrated Liquid Water (ILW)

As mentioned in the introduction, the radiometers also measure ILW. For that reason, these measurements were compared similarly to the method described in Sec. 3.3. Whereas the TP/WVP-3000 does not deliver negative ILW values due to the neural network algoritm (WARE et al. (2003)), the ASMUWARA ILW retrieval algorithm (MARTIN et al. (2006b)) can produce slightly neg-

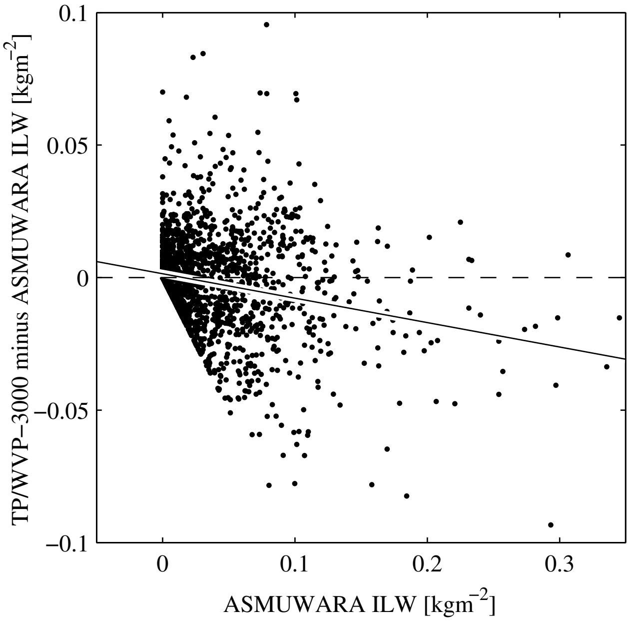

Figure 7: TP/WVP-3000 derived ILW minus ASMUWARA derived ILW. Numerical values are given in Table 4.

	TP/WVP-3000
samples	3072
mdiff [kgm^{-2}]	0.0005
std [kgm^{-2}]	0.015
mstd [kgm^{-2}]	0.007
corr	0.92
slope	−0.09

Table 4: Numerical values to Fig. 7. samples: number of samples; mdiff: mean difference; std: standard deviation; mstd: mean std of all averaging intervals; slope: slope of fitted straight line; corr: correlation coefficient.

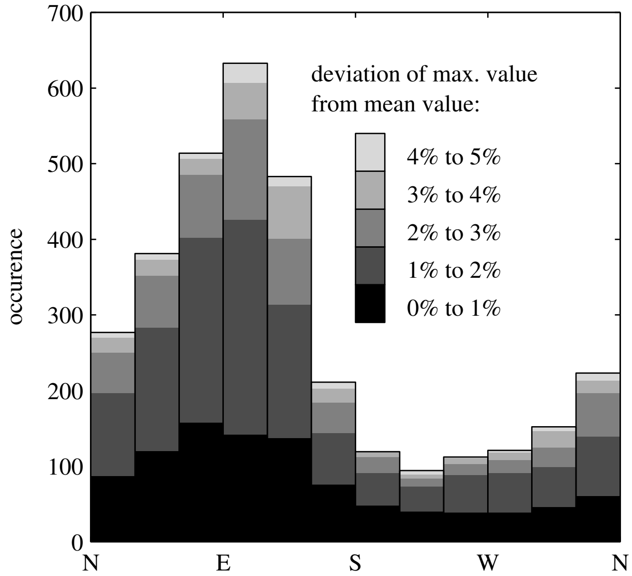

Figure 8: Histogram of the direction of the maximum IWV value measured with the ASMUWARA radiometer during the whole TUC campaign. The grey scale quantifies how much the maximum value exceeds the mean value.

θ [°]	a	b	c
0			0.19
15	−0.12%	−0.18%	0.18
30	−0.30%	−0.38%	0.17
40	−0.31%	−0.39%	0.17
50	−0.40%	−0.50%	0.16
60	−0.39%	−0.66%	0.17
70	0.35%	0.24%	0.29

Table 5: Tests of IWV zenith angle (θ) dependence: a: deviation of zenith mapped non-zenith IWV from zenith IWV [% of zenith value], single values. b: same as a but hourly averages. c: mean hourly standard deviation of IWV [kgm^{-2}].

ative values. To have an equal database, negative ASMUWARA ILW values were therefore set to zero. The comparison (Fig. 7 and Table 4) shows no significant mean difference between the ILW measurements of the two radiometers. However, the scatter is considerable. It is most probably due to the highly variable cloud structure in combination with the sampling mismatch caused by the horizontal distance between the radiometers of approx. 200 m, by the different beamwidth, and by the different temporal resolution of the radiometers. The slope of the fitted straight line is slightly negative, but it should be taken into account that the linear regression is strongly influenced by the large number of measurements close to zero.

4 Analysis of systematic error sources

Several tests were made to spot systematic errors in the IWV database. ASMUWARA makes measurements in all directions of the sky allowing assessment of the effect of IWV inhomogeneities. The ASMUWARA observation pattern includes an azimuthal scan where IWV measurements in 30° steps are made under a zenith angle of 60°. Sinus functions were fitted in each of these scans to detect the direction of the maximum value (MARTIN (2003)). A histogram of this analysis is shown in Fig. 8. The histogram clearly shows that the maximum IWV is mostly in E direction and that the maximum value exceeds the mean value of all directions by typically less than 2%. However, it is likely that this effect is due to insufficient levelling of ASMUWARA. A misalignment of 0.7° is enough to cause an IWV excess of 2%, and the instrument could be levelled to an accuracy of ±0.5°. Furthermore, the platform where ASMUWARA was mounted during the TUC campaign was not very stable.

The tipping scans made with ASMUWARA were used to find out if the IWV measurements depend on the zenith angle. The results of those tests are summarised in Table 5. In column a, the mean relative difference of zenith mapped non-zenith IWV measurements with respect to the zenith value is given. Data from the whole

TUC campaign measured in all directions of the sky (except W) were considered. It is seen that the deviation of non-zenith measurements from zenith measurements is small on average. The same is true if the data are averaged over one hour (column *b*). In column *c* the mean hourly std of zenith mapped IWV measurements is given. It is seen that the mean std is smallest for measurements made under a zenith angle of 50°. This indicates that IWV measurements made at this angle have the potential to enhance the signal-to-noise ratio.

All intercomparisons described in Sec. 3 (excepting the ILW comparison) were also made under exclusion of clouds, i. e. cases with ILW smaller than 0.03 kgm^{-2}. Since no significant discrepancies occurred, details of these tests are not shown.

5 Conclusions

IWV measurements made with SRS 400 radiosondes, GPS meteorology, and TP/WVP-3000 and ASMUWARA microwave radiometers were compared based on a campaign made during three months under mid-latitude winter conditions. The results of the intercomparison show clearly that the general agreement is good, and that discrepancies are mainly due to inherent limitations of the different methods. The comparison of the radiosonde IWV with the remotely sensed IWV yields only a small bias (except for the GPS measurement), but has a std of almost 1 kgm^{-2}. This is most probably due to the different temporal and spatial sampling of the methods. Whereas the radiosonde produces a snapshot of water vapour integrated along its ascent path, the GPS measurement yields hourly IWV averages of almost the whole upper hemisphere, and the radiometers continuously sample a 5.5°- or 8.5°-taper in zenith direction. In the comparison of GPS IWV with the radiometric IWV, hourly averages are applied leading to a better averaging of temporal inhomogeneities. This results in a std of approx. 0.7 kgm^{-2}. The std of the IWV difference between the radiometers based on thirty-minute averages is only 0.37 kgm^{-2} being most probably due to the coinciding observation geometry and to the identical measuring method. However, with respect to the more variable ILW, the scatter is considerable.

The GPS retrieved IWV has a persistent dry bias of approx. 0.5 kgm^{-2} in comparison with radiosondes and radiometers. Furthermore the GPS method tends to overestimate high IWV values and underestimate low IWV values. A characteristic diurnal cycle of the IWV was identified. The mean difference between radiosonde and TP/WVP-3000 IWV is 0.11 kgm^{-2}, and the difference between radiosonde and ASMUWARA IWV is -0.12 kgm^{-2} being not significant for both radiometers with respect to the double standard error. The mean difference between ASMUWARA and TP/WVP-3000 IWV based on 3072 thirty-minute samples is 0.14 kgm^{-2}. ASMUWARA tends to overestimate high IWV values and to underetimate low IWV values with respect to all other sensors. This was due to radiometric non-linearities which were eliminated after the TUC campaign. Tipping scans made with ASMUWARA showed that the mean difference between zenith and non-zenith IWV measurements is below 0.4%. However, the signal-to-noise ratio is best at a zenith angle of 50° due to greater atmospheric path lengths.

Acknowledgements

This publication was enabled and encouraged by Prof. Dr. N. Kämpfer, University of Bern, Switzerland. Funding was provided by the Swiss National Science Foundation (grant 200020-107665), by NCCR Climate, by COST 720 and by armasuisse.

References

BEVIS, M., S. BUSINGER, T. A. HERRING, C. ROCKEN, R. A. ANTHES, R. H. WARE, 1992: GPS Meteorology: Remote Sensing of Atmospheric Water Vapor Using the Global Positioning System. J. Geophys. Res. **97**(D14), 15787–15801.

CIMINI, D., T. J. HEWISON, L. MARTIN, J. GÜLDNER, C. GAFFARD, F. S. MARZANO, 2006: Temperature and humidity profile retrievals from ground-based microwave radiometers during TUC. Meteorol. Z. **XX**(XX), XX–XX.

ELGERED, G., B. O. RÖNNÄNG, J. I. H. ASKNE, 1982: Measurements of atmospheric water vapor with microwave radiometry. Radio Sci. **1**(5), 1258–1264.

EMARDSON, T. R., G. ELGERED, J. M. JOHANSSON, 1998: Three months of continuous monitoring of atmospheric water vapor with a network of Global Positioning System receivers. J. Geophys. Res. **103**(D2), 1807–1820.

FUJIWARA, M., M. SHIOTANI, F. HASEBE, H. VÖMEL, S. J. OLTMANS, P. W. RUPPERT, T. HORINOUCHI, T. TSUDA, 2003: Performance of the Meteolabor “Snow White” Chilled-Mirror Hygrometer in the Tropical Troposphere: Comparisons with the Vaisala RS80 A/H-Humicap Sensors. J. Atmos. Ocean. Technol. **20**(11), 1534–1542.

GUEROVA, G., J.-M. BETTEMS, E. BROCKMANN, C. MATZLER, 2005: Assimilation of COST 716 Near-Real Time GPS data in the nonhydrostatic limited area model used at MeteoSwiss. Meteorol. Atmos. Phys. .

KNEIZYS, F. X., L. W. ABREU, G. P. ANDERSON, J. H. CHETWYND, E. P. SHETTLE, A. BERK, L. S. BERNSTEIN, D. C. ROBERTSON, P. ACHARYA, L. S. ROTHMAN, J. E. A. SELBY, W. O. GALLERY, S. A. CLOUGH, 1996: The MODTRAN 2/3 Report and LOWTRAN 7 Model. Tech. rep., Ontar Corporation, 9 Village Way, North Andover, MA 01845, U.S.A.

KOPKEN, C., 2001: Validation of integrated water vapor from numerical models using ground-based GPS, SSM/I, and water vapor radiometer measurements. J. Appl. Meteorol. **40**(6), 1105–1117.

LIOU, Y.-A., Y.-T. TENG, T. V. HOVE, J. C. LILJEGREN, 2001: Comparison of Precipitable Water Observations in the Near Tropics by GPS, Microwave Radiometer, and Radiosondes. J. Appl. Meteorol. **40**(1), 5–15.

MARTIN, L., 2003: Microwave Transmission and Emission Measurements for Tropospheric Monitoring. Inauguraldissertation der Philosophisch-naturwissenschaftlichen Fakultät, Institut für Angewandte Physik Universität Bern, Bern, Switzerland.

MARTIN, L., M. SCHNEEBELI, C. MÄTZLER, 2006a: ASMUWARA, a ground-based radiometer system for tropospheric monitoring. Meteorol. Z. **XX**(XX), XX–XX.

———, 2006b: Tropospheric water and temperature retrieval for ASMUWARA. Meteorol. Z. **XX**(XX), XX–XX.

NIELL, A. E., 1996: Global mapping functions for the atmosphere delay at radio wavelengths. J. Geophys. Res. **101**(B2), 3227–3246.

REVERCOMB, H. E., D. D. TURNER, D. C. TOBIN, R. O. KNUTESON, W. F. FELTZ, J. BARNARD, J. BÖSENBERG, S. CLOUGH, D. COOK, R. FERRARE, J. GOLDSMITH, S. GUTMAN, R. HALTHORE, B. LESHT, J. LILJEGREN, H. LINNÉ, J. MICHALSKY, V. MORRIS, W. PORCH, S. RICHARDSON, B. SCHMID, M. SPLITT, T. V. HOVE, E. WESTWATER, D. WHITEMAN, 2003: The ARM Program's Water Vapor Intensive Observation Periods. Bull. Am. Meteorol. Soc. **84**(2), 217–236.

RICHNER, H. (Ed.), 1999: Grundlagen aerologischer Messungen speziell mittels der Schweizer Sonde SRS 400. Veröffentlichungen der SMA–MeteoSchweiz, No. 61, SMA–Meteo Schweiz.

RUFFIEUX, D., J. NASH, P. JEANNET, J. L. AGNEW, 2006: The COST 720 temperature, humidity, and cloud profiling campaign: TUC. Meteorol. Z. **XX**(XX), XX–XX.

TREGONING, P., R. BOERS, D. O'BRIEN, M. HENDY, 1998: Accuracy of absolute precipitable water vapor estimates from GPS observations. J. Geophys. Res. **103**(D22), 28701–28710.

VÖMEL, H., M. FUJIWARA, M. SHIOTANI, F. HASEBE, S. J. OLTMANS, J. E. BARNES, 2003: The Behavior of the Snow White Chilled-Mirror Hygrometer in Extremely Dry Conditions. J. Atmos. Ocean. Technol. **20**(11), 1560–1567.

WANG, J., L. ZHANG, A. DAI, 2005: Global estimates of water-vapor-weighted mean temperature of the atmosphere for GPS applications. J. Geophys. Res. **110**(D21101).

WARE, R., R. CARPENTER, J. GÜLDNER, J. LILJEGREN, T. NEHRKORN, F. SOLHEIM, F. VANDENBERGHE, 2003: A multichannel radiometric profiler of temperature, humidity, and cloud liquid. Radio Sci. **38**(4), 44.1–44.13.